Fluorescence of guest molecules in a scattering state of a liquid crystal

A. Hochbaum, L. J. Yu,[a] and M. M. Labes
Departments of Physics and Chemistry, Temple University, Philadelphia, Pennsylvania 19122

(Received 8 August 1979; accepted for publication 3 October 1979)

Fluorescence emission of guest molecules in cholesteric liquid crystal hosts was modulated by an electric-field-induced cholesteric-nematic transition. The contrast ratio between the two states can be greater than 15, and is affected primarily by the scattering properties of the phase and the order parameter of the guest. Data are presented on the dependence of the contrast ratio on the cell parameters and the structure of both guest and host. A simple model is presented accounting for the observed behavior.

PACS numbers: 33.50. – j, 61.30.Gd, 85.60.Pg

INTRODUCTION

The concept of controlling the fluorescence emitted from a liquid crystal containing a fluorescent guest molecule by electrically switching from a scattering cholesteric texture to a nonscattering nematic texture has recently been demonstrated.[1] The initial study of this effect utilized as a guest a brilliant red fluorescent rare-earth chelate, europium thenoyltrifluoroacetonate (EuTTA), emitting at 612 nm, with essentially no polarization of its emission or absorption (excitation maximum ~360 nm). Thus, the large contrast between the intense emission in the cholesteric state and the weak emission in the homeotropic nematic state must be associated with the difference in scattering between the two textures. It can be enhanced if one employs a fluorescent guest with a nonvanishing order parameter. In this work several guest materials are employed of different degrees of polarization, and the dependence of the observed contrast ratio (CR) is discussed in terms of various system parameters. A model attributing the observed CR primarily to multiple scattering is presented.

EXPERIMENTAL

As host materials, we employed a mixture of benzoyloxybenzoate esters obtained from Hoffman-LaRoche (Nematic Mixture A—RO-TN-100), *p*-pentylphenyl-2-chloro-4-(*p*-pentylbenzoyloxy) benzoate (BOB) obtained from Eastman Kodak, and *p*-cyano-*p'*-pentylbiphenyl (CPB) obtained from British Drug House. Most of the work was done in a cholesteric phase made by doping Nematic Mixture A with cholesteryl nonanoate (CN). The pitch p of these mixtures was determined from the measured distances between Grandjean lines in a wedge-type cell.[2] These cholesteric hosts have a positive dielectric anisotropy, so that application of a field to a cholesteric sample in the focal conic texture, which is strongly scattering, causes the sample to switch to a nonscattering homeotropic texture.

The fluorescent guest molecules employed are listed in Table I. With the exception of CPB, the cholesteric hosts are transparent in the uv. Samples were prepared using Mylar spacers between untreated tin-oxide-coated conducting glass plates. In all cases, the homeotropic configuration was induced by applying an ac 1-kHz field $E \sim 1.5E_c - 2E_c$, where E_c is the threshold field[3] needed to fully unwind the cholesteric. When the pitch is very small ($\sim 0.5\,\mu$m), $E_c \sim 10^5$ V cm^{-1}. In order to lengthen the relaxation process, bias fields $E_b \sim 0.2E_c$ at 100 Hz were applied in some of the measurements. Figure 1 indicates the fluorescence emission in

TABLE I. Maximum wavelength of excitation and fluorescence of guests and hosts.

Guest	Max. excitation (nm)	Max. fluorescence (nm)
EuTTA [a]	350	612
Eu(BTFA)$_4$·P_{γ} [b]	350	612
Eu (mixed ligands) [c]	350	612
p-quinquephenyl	365	429
Host		
CPB	340	370
BOB	...	...
A	...	...
CN	...	...

[a]TTA = thenoyltrifluoroacetonate trihydrate.
[b](BTFA)$_4$·P_{γ} = tetrakisbenzoyltrifluoroacetonate pyrrolidinium salt.
[c]Mixed ligands = 2,4-pentanedione + TTA in 2 : 1 ratio.

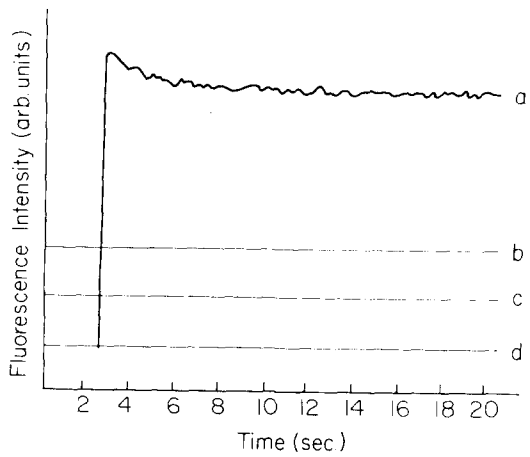

FIG. 1. Comparison of fluorescence intensity in various configurations of a typical sample: 0.23 wt% *p*-quinquephenyl in CN-A mixture, 23 μm thick. (a) Switching from homeotropic to the scattering state followed by relaxation under a bias field. (b) Planar cholesteric. (c) Isotropic phase. (d) Homeotropic configuration.

[a]Present address: Liquid Crystal Institute, Kent State University, Kent, Ohio.

 0021-8979/80/020867-06$01.10

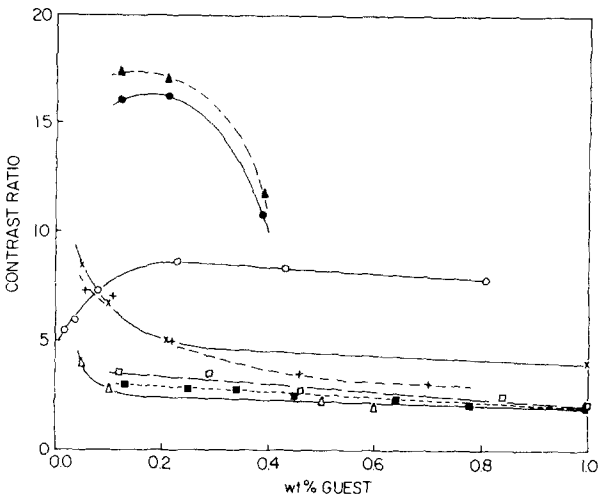

FIG. 2. Contrast ratio as a function of wt% of various guests in different cholesteric-nematic matrices. ▲, with and ●, without bias for *p*-quinquephenyl in CN-A, $p = 0.52\,\mu$m, thickness = $12.7\,\mu$m; ○, *p*-quinquephenyl in CN-CPB, $p = 0.6\,\mu$m, thickness = $12.7\,\mu$m; ×, EuTTA in CN-CPB, $p = 0.6\,\mu$m, thickness = $23.4\,\mu$m; +, EuTTA in CN-CPB, $p = 0.7\,\mu$m, thickness = $23.4\,\mu$m; △, EuTTA in CN-CPB, $p = 1.6\,\mu$m, thickness = $23.4\,\mu$m; □, $Eu(BTFA)_4 \cdot P_1$ in CN-CPB, $p = 0.6\,\mu$m, thickness = $12.7\,\mu$m; ■, Eu (mixed ligands) in CN-CPB, $p = 0.6\,\mu$m, thickness = $12.7\,\mu$m.

different configurations for the guest molecule *p*-quinquephenyl in Mixture A-CN.

The samples were electrically switched by a microswitch between the homeotropic configuration with low fluorescent intensity to a scattering state at the off field state with higher fluorescent intensity. The ratio of these intensities is the measured CR. CR's were measured at the maximum fluorescent wavelength of the emitter, and refer to the maximum fluorescent intensity observed during the relaxation process. Fluorescence intensity was measured in the transmission mode of the experimental arrangement previously described.[1]

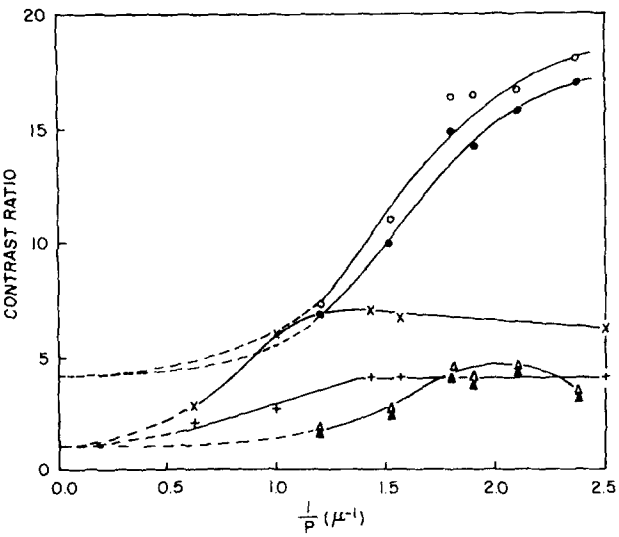

FIG. 3. Contrast ratio as a function of reciprocal pitch. ○, with and ●, without bias for 0.2 wt% of *p*-quinquephenyl in CN-A, thickness = 12.7 μm; ×, 0.1 wt% and +, 0.5 wt% of EuTTA in CN-CPB, thickness = 23.4 μm; Δ, with and ▲, without bias for 0.2 wt% of $Eu(BTFA)_4 \cdot P_1$ in CN-A, thickness = 12.7 μm.

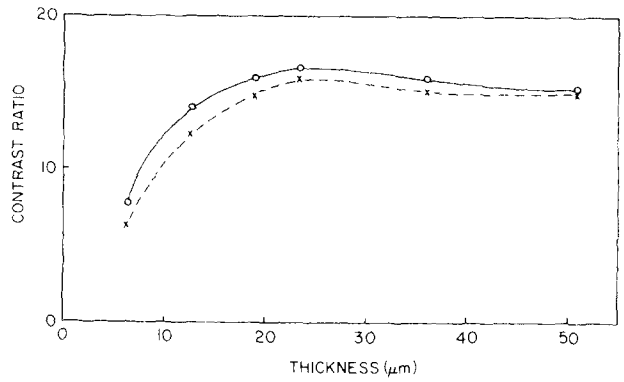

FIG. 4. Contrast ratio as a function of sample thickness. 0.2 wt% of *p*-quinquephenyl in CN-A, $p = 0.52\,\mu$m. ○, with bias voltage; ×, without bias voltage.

The dependence of CR on guest concentration in various hosts is presented in Fig. 2. The general trend of these data indicates that CR increases with decreasing guest concentration. One exception is the data on CPB-CN containing low guest concentrations of *p*-quinquephenyl. This behavior is due to the superposition of some CPB emission on the guest emission. The fluorescent emission peak of CPB is at 370 nm, whereas the guest emission of *p*-quinquephenyl peaks at 429 nm.

The variation of CR with pitch and cell thickness is given in Figs. 3 and 4, respectively. CR increases with decreasing pitch and with increasing cell thickness, saturating at about $20\,\mu$m. The pitch dependence data do not show any peak which might be associated with selective reflection of exciting or emitted light. The CR's are higher for the guest *p*-quinquephenyl because of the strong polarization of its fluorescence. Data on polarization ratios were measured in the host BOB by comparing emission in the homogeneous and homeotropic configuration, and are presented in Table II. Homogeneous alignment was achieved by evaporating silicon monoxide onto the conducting glass substrates.[4]

DISCUSSION

The observed fluorescence CR has contributions from the differences in the absorption (ACR) and in the emission (ECR) between the off-on states, such that

$$CR \approx ACR \cdot ECR.$$

White and Taylor[5] have shown that in a guest-host effect[6] using a planar cholesteric as a host, the absorption of

TABLE II. Polarization ratio of fluorescence of two guests in nonfluorescent BOB. Sample thickness: 50.8 μm.

	Homogeneous alignment [a]	Homogeneous/ homeotropic [b]
0.2 wt% *p*-quinquephenyl	4.7 ± 0.3	4.2 ± 0.3
0.7 wt% $Eu(BTFA)_4 \cdot P_1$	1.4 ± 0.1	1.14 ± 0.05

[a] A polarizer between the sample and the detector was switched between ∥ and ⊥ direction with respect to the director alignment.
[b] The director alignment was switched by an electric field between homogeneous and homeotropic configurations.

unpolarized light is enhanced in the off state. The reason is that both elliptically polarized modes of the incident light are absorbed by the dichroic dye in the planar cholesteric configuration. This model or similar models of improved absorption in the off state, compared to the on state, which neglect the effect of scattering cannot by themselves explain the data. Such a model predicts:

$$\mathrm{ACR} = \frac{1 - \exp[-K(1-S)\alpha_0 d]}{1 - \exp[-(1-S)\alpha_0 d]}, \qquad (1)$$

where S is the order parameter of the dye, α_0 is the absorption coefficient in an isotropic sample, d is the cell thickness, and $K = (2+S)/(2-2S)$ for optimal absorption in a cholesteric host, or $K = 1/(1-S)$ in the scattering state.[5] The ECR is not expected to depend on the cell's parameters. The CR dependence on the parameter is therefore obtained from Eq. (1), which predicts that the CR is a decreasing function of thickness. This is not consistent with the observed behavior. Equation (1) cannot explain the parameters' dependence of the CR in the EuTTA samples where $S = 0$. Equation (1) also predicts a higher CR in the planar cholesteric cell than in the scattering cell, in contrast with the behavior shown in Fig. 1. Nor can the data be accounted for adequately by considering the lengthening of the uv effective path by the diffraction action of the focal-conic configuration.[7] We observed a diffraction pattern of a He-Ne laser beam only in a narrow range in the relaxation process of the scattering state with a static bias field, while the fluorescent signal did not show this transient behavior (Fig. 1). From microscopic observations of the scattering state we found that the configuration with the most efficient diffraction action is of a larger domain size than that which gives the maximum in the fluorescence signal. Previous measurements[8] of the angular distribution of the scattered light intensity from the focal-conic configuration indicate that selective reflection by the periodic structure of the cholesteric is a secondary effect superimposed on a narrow scattering peak, and cannot be considered to be important in lengthening the uv average path in the cell.

We propose multiple scattering of the uv to be the primary effect. This process is responsible for the increase of the average uv path, and for the emission of most of the visible light through the two large surfaces of the cell. In this model, the cholesteric pitch controls the dimension of the scattering

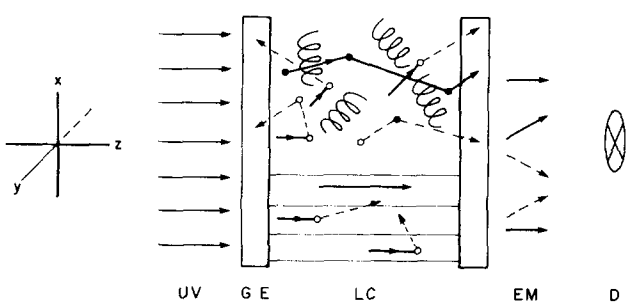

FIG. 5. Visualization of the absorption process. UV—collimated uv beam, G—glass plate; E—transparent electrode; LC—cholesteric liquid-crystal layer in a scattering state (top) and homeotropic state (bottom); EM—emission radiation; D—detector; ●—scattering event; ○—emission event.

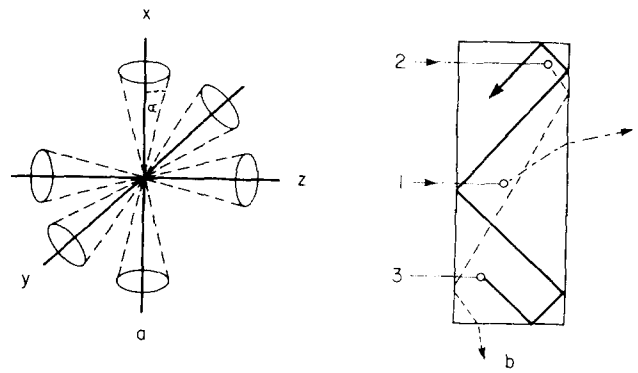

FIG. 6. Visualization of the emission process. (a) Emission cones, $\alpha = \sin^{-1}(n_{\mathrm{glass}}^{-1})$. (b) Examples of emission through the z cone (1), x cone (2), and a trapped beam (3).

domains. We neglect the helical inner structure of the domains, except for its function of randomizing the direction of the absorption and emission dipoles.

Our samples consist of a thin cholesteric layer with thickness $d \sim 20\,\mu$m bounded by two glass plates ~ 1 mm thick perpendicular to the z axis along which a collimated uv beams propagates (Fig. 5). The dependence of the transmitted intensity on thickness in a wedge-type cell, homogeneously aligned with 0.12 wt% of EuTTA, was measured. By fitting the data to an exponential decay, the absorption length was estimated to be $a = 115 \pm 10\,\mu$m at $\lambda = 350$ nm; thus, for low concentrations we assume $a \gg d$. We denote the complex index of refraction of the isotropic guest-host mixture by $n_{\mathrm{LC}} = n_0(1 - ix)$, and the above typical value of a indicates that $x \ll 1$. With the assumption that $(n_{\mathrm{glass}} - n_0)/n_0 \ll 1$, we can safely neglect reflections between the LC layer and the glass. We thus can treat the sandwich-type cell as one slab with a very thin inner layer that absorbs, fluoresces, and is switched between scattering and nonscattering states. The liquid-crystal layer is characterized by its thickness d, by guest concentration or absorption length a, and by a scattering length l. The scattering length is reduced by decreasing the pitch and is expected to be of the order p. In our experiments, the absorption length varies between $a \gg d$ to $a \simeq d$, and the scattering length is assumed to vary between $l \simeq d$ to $l < d$.

The emission phenomenon from fluorescent centers embedded in a transparent slab was analyzed[9] in the following way: Each emission center is associated with six cones, each perpendicular to one of the cell surfaces, with an apex angle $\alpha = \sin^{-1}(n_{\mathrm{glass}}^{-1})$ [Fig. 6(a)]. Rays propagating from such a center in a direction within one of the cones are emitted through the corresponding surface, while rays propagating outside the cones are trapped by total reflection. The emissions from all surfaces are equal. In our case, the two z surfaces are much larger than the side surfaces [Fig. 6(b)]. Therefore, the average path of a ray emitted through a z surface is of the order d. This path is much shorter than the average path of a ray emitted through a side surface, usually after a sequence of total reflections from the z surfaces. If a scattering state is introduced, the trapped light and rays propagating within the x,y cones, which traverse the scatter-

ing layer many times, have a high probability of being scattered and eventually exiting through the z surfaces. The distribution of the emitted light does not depend on d or a. For a scattering length shorter than d, it is plausible to assume that most of the visible light is emitted through the z surfaces, and a further decrease of l will have a negligible effect on the emission process. We assume, therefore, that the emission characteristics of the scattering configuration is independent of the cell's parameters.

In the scattering state, the angular distribution of the emitted light is uniform within the z cones inside the glass and is given by:

$$I_s = (I_0/4\pi)\ [1/(1-\cos\alpha)], \tag{2}$$

where I_0 is the total intensity of the emitted light. In the case of an isotropic emitter like EuTTA, the angular distribution of the intensity in the homeotropic state is as follows:

$$I_{\rm iso} = I_0/4\pi. \tag{3}$$

A detector perpendicular to the z axis will observe:

$$\mathrm{ECR} = [1/(1-\cos\alpha)]. \tag{4}$$

For $n_{\rm glass} = 1.5$, one therefore expects ECR$\simeq$3.9.

If the emission dipoles are oriented preferentially with the nematic director, as in the case of p-quinquephenyl, then the angular distribution of the intensity inside the glass is given by:

$$I(\theta) = \frac{3I_0}{8\pi}\left(\frac{2-2S}{3} + S\sin^2\theta\right), \tag{5}$$

when the detector samples only a small solid angle around the θ direction. The angle θ is measured from the direction of the nematic director, no polarizers are used, and one assumes that the anisotropy in the nematic refractive index is small. In the homeotropic case, θ is measured from the z axis, and the ECR for an aligned emitter is given by:

$$\mathrm{ECR} = \frac{1}{(1-\cos\alpha)(1-S)}. \tag{6}$$

The order parameter of p-quinquephenyl was estimated, from the measurement of the dichroic ratio,[5] to be $S = 0.5 \pm 0.05$. Using Eq. (6), we expect, therefore, ECR$\simeq$7.8 for the p-quinquephenyl cells.

In practical cells, very efficient scattering occurs at the periphery of the cell from imperfection of the side walls and the spacers. This by itself would not reduce the ECR in the middle of the cell. It is the presence of homogeneously distributed impurities and undissolved guest particles, even at low guest concentration, that scatters light from side cones and trapping directions into the z cones in the homeotropic configuration. It is this scattering, together with the peripheral scattering, which is responsible for a reduction of the ECR. If only the weak scattering from suspended particles would be present, all the trapped light would still be scattered into the emission cones. Assuming this scattering to be isotropic, the scattering of trapped light only would reduce the ECR to a value of 3 for an isotropic emitter and to 4.5 for an aligned emitter with $S = 0.5$. The relative reduction of the ECR is more significant for the aligned emitter, since in the homeotropic case the emission intensity distribution reaches a maximum for $\theta = \frac{1}{2}\pi$ [Eq. (5)]. For high guest concentrations $a \sim d$, one expects ACR$\simeq$1, and thus the saturation values of the curves in Fig. 2 are essentially the ECR, which is about 3 for the isotropic EuTTA and about 7 for p-quinquephenyl. On the basis of this model for the emission, we expect CR > 1 even when $S = 0$ or at high concentrations. The CR will increase with increasing S. These predictions are supported by the data in Figs. 2–4.

In order to understand the dependence of the CR on the cell parameters and the observation of CR values that cannot be explained by the ECR alone, let us analyze the ACR of an isotropic emitter in terms of a simple model. Referring to Fig. 5, we assume that a collimated uv beam of intensity I_c propagates along the z axis, perpendicular to the glass plates. In the scattering state, light is eliminated from the collimated beam by direct absorption and by scattering off the $+z$ direction. The direct absorption is given by:

$$A_c = \frac{lI_c}{a+l}\left\{1 - \exp\left[-\left(\frac{1}{l}+\frac{1}{a}\right)d\right]\right\}. \tag{7}$$

The absorption from the diffused light is given by:

$$A_d = \frac{\beta a I_c}{a+l}\left\{1 - \exp\left[-\left(\frac{1}{l}+\frac{1}{a}\right)d\right]\right\}, \tag{8}$$

where β denotes the fraction of the diffused light that has been absorbed. In the homeotropic configuration, there is only a contribution from direct absorption,

$$A_h = I_c[1 - \exp(-d/a)]. \tag{9}$$

The ACR is thus given by:

$$\mathrm{ACR} = \frac{A_c + A_d}{A_h} = \frac{\beta a/d + l/d}{a/d + l/d}\,\frac{1 - \exp[-(1/l + 1/a)d\ ]}{1 - \exp(-d/a)} \tag{10}$$

β is, of course, a complicated function of the various characteristic lengths. Nevertheless, we will try to estimate its gross features. At a fixed scattering length, $l < d$, one expects at very low concentrations, where $a \gg d$, that $\beta \ll 1$, while at very high concentrations, where $a \sim d$, that $\beta \sim 1$. At a fixed absorption length $a > d$, we expect $\beta \ll 1$ when $l > d$, since the probability for multiple scattering is very low. Also, we expect $\beta \ll 1$ for $l \ll d$, where the reflectivity of the cell is near unity as the light diffuses only into a very thin layer and

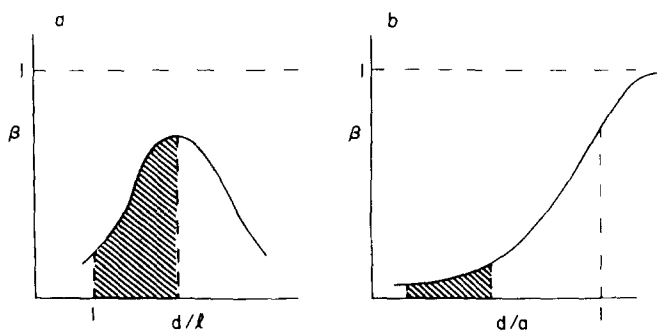

FIG. 7. Qualitative behavior of β as a function of: (a) the scattering length l and (b) the absorption length a ($l < d$). The shaded areas are the probable range of cell parameters in the experiments.

has a small average path in the absorbing media. Nevertheless, we expect to obtain a finite maximum for intermediate values of l. Thus, $\beta = \beta(d/l, d/a)$ is expected to behave roughly as indicated in Figs. 7(a) and 7(b). The shaded areas are the assumed ranges of the parameters in our experiments. We assume that within the experimental range, β is more sensitive to changes in the scattering length than to the concentration:

$$\frac{\partial\beta}{\partial(d/l)} \sim 1 \gg \frac{\partial\beta}{\partial(d/a)}. \tag{11}$$

Based on these plausible assumptions, we can use Eq. (10) to estimate the ACR dependence on various parameters.

Thickness dependence

For a very thin cell, $d = l$, with a fixed pitch and low concentration such that $a \gg l$, Eq. (10) can be reduced to:

$$\mathrm{ACR} \simeq (1 + \beta a/l)\,\frac{1 - \exp(-d/l)}{d/l} \tag{12}$$

At these thicknesses, we see that the ACR is a rapidly increasing function of thickness (measured in units of l) with a rate $\beta a/l > 1$, which is indeed what is observed experimentally (Fig. 4).

In very thick cells where $d \simeq a$, the ACR can be approximated by:

$$\mathrm{ACR} \simeq \frac{\beta}{1 - \exp(-d/a)}. \tag{13}$$

When $d \gg l$, β is saturating or decreasing rapidly [Fig. 7(a)], and one expects from Eq. (13) that the ACR will saturate as is observed in our data.

Concentration dependence

Keeping the pitch and thickness fixed, $d > l$, and reducing the concentration to the range $a \gg d$ allows us to approximate Eq. (10) by:

$$\mathrm{ACR} \simeq (\beta a/d + l/d)\,[1 - \exp(-d/l)]. \tag{14}$$

As β is a slowly decreasing function of a/d [Eq. (11)], the term $\beta a/d$ is expected to increase the ACR at lower concentrations. This increase is indeed observed in the experiments (Fig. 2).

Pitch dependence

Decreasing the pitch is expected to increase the mixed factor $\beta a/d + l/d$ in Eq. (10) as $a > d$. All the other terms clearly contribute to an increase in the ACR. This behavior at low concentration is observed in Fig. 3.

The above model assumed an isotropic distribution of the absorbing dipoles. For samples with an aligned guest, the absorption length in the homeotropic state is Ka, where $K = \frac{1}{3}(2 + a_\perp/a_\parallel) > 1$, $a_\parallel$ and $a_\perp$ are the absorption lengths in the homogeneous and homeotropic configurations, and each is related to a by the order parameter[5] S such that $a_\perp/a_\parallel = (2S+1)/(1-S)$. The absorption length in the scattering state is a, as in the isotropic state, even for an aligned absorber.[5] For most of our experiments, we can make the approximation $1 - \exp(-d/Ka) \simeq d/Ka$, and thus the effect of a nonvanishing order parameter is to increase the ACR by a factor K as compared to an equivalent fluorescent molecule unaligned in its ground state. This expected increase of the CR is shown in the data in Figs. 2 and 3. For an efficient scattering host $l < d$ with high guest concentration $a \sim d$, it is possible to estimate the quantity:

$$R = \frac{\mathrm{CR}\,(S \neq 0)}{\mathrm{CR}\,(S = 0)}. \tag{15}$$

Depending on whether $[(1-S)d]/a \lesssim 1$, one expects the values of R to be distributed in the range $(1-S)^{-1} \lesssim R \lesssim (1-S)^{-2}$. For p-quinquephenyl we expect $2 \lesssim R \lesssim 4$, which agrees with the high concentration data in Fig. 2.

It is clear from Fig. 2 that there is a tradeoff between CR and brightness. Very high concentrations will reduce the CR to its lower limit. We have found that a substituted quaterphenyl is very soluble in liquid crystals. Nevertheless, cells with high concentration of this material gave a small CR. Thus, selection of the appropriate guest molecule is very important. Only very efficient fluorescent materials which are reasonably soluble and have high-order parameters will provide sufficient brightness and reasonable CR.

Liquid crystals offer other scattering configurations than the cholesteric focal conic texture investigated in this work. Switching a nematic cell between homeotropic and dynamic scattering states has the advantage that one can increase continuously the ratio d/l by increasing the voltage.[10] We indeed observed an increase in the CR with the voltage across the cell but the numerical values of the CR were low. It is possible that the presence of currents at low frequency might be responsible for quenching the fluorescence in the scattering state.[11]

Elimination of suspended particles and using absorbing spacers and side walls are also expected to improve the CR. We attempted to increase the CR by increasing the probability of the scattering of the uv and thereby achieving a longer average path; but in each scattering event, most of the scattered light was scattered within a narrow cone around the forward direction. If one could widen this distribution continuously or obtain a very efficient large-angle selective reflection, one would expect a significant increase in the ACR. Another scheme that has the potential of increasing the ACR is to embed the uv source in the liquid-crystal layer itself. This could be done, for example, by dissolving another guest molecule that absorbs in the short uv and emits in a region which overlaps the absorption of the primary fluorescent guest.

ACKNOWLEDGMENTS

This work was supported by the Army Research Office (Durham) under Grant No. DAAG29-78-G-0001. We thank Dr. D. Dalton and A. Langman for synthesis of some of the europium chelates, and Hoffman-LaRoche for furnishing Nematic Mixture A.

[1] L.J. Yu and M.M. Labes, Appl. Phys. Lett. **31**, 719 (1977).
[2] R. Cano, Bull. Soc. Franc. Mineral. Crist. **91**, 20 (1968).

[3]R.B. Meyer, Appl. Phys. Lett. **14**, 208 (1968).
[4]L.J. Janning, Appl. Phys. Lett. **21**, 173 (1973).
[5]D.L. White and G.N. Taylor, J. Appl. Phys. **45**, 4718 (1974).
[6]G.H. Heilmeier and L.A. Zanoni, Appl. Phys. Lett. **13**, 91 (1968).
[7]N.L. Kramarenko, I.V. Kurnosov, and Yu. V. Naboikin, Mol. Cryst. Liq. Cryst. **47**, 7 (1978).
[8]D. Meyerhofer and E.F. Pasierb, Mol. Cryst. Liq. Cryst. **20**, 279 (1973); M. Kawachi, K. Kato, and O. Kogure, Jpn. J. Appl. Phys. **17**, 1245 (1978).
[9]W.A. Shurcliff and R.C. Jones, J. Opt. Soc. Am. **39**, 912 (1949).
[10]P. Stepanek and B. Sedlacek, Mol. Cryst. Liq. Cryst. **43**, 197 (1977).
[11]D.P. Hamblen and J.R. Clarke, IEEE Trans. Electron. Devices **ED-20**, 1028 (1973).